Search for nonresonant capture in the $^{16}O(\alpha,\gamma)^{20}Ne$ reaction at low energies

K. H. Hahn,* K. H. Chang,† T. R. Donoghue,‡ and B. W. Filippone
California Institute of Technology, Pasadena, California 91125
(Received 25 March 1987)

^{20}Ne recoils produced from the $^{16}O(\alpha,\gamma)^{20}Ne$ reaction were detected in coincidence with capture γ rays using a recoil separator, NaI(Tl) γ-ray detectors, and a helium gas target. Total cross sections for cascade and ground state capture were measured in the range $E_{c.m.}=1.7$–2.35 MeV. Improved measurements of the total width and resonance strength of the $E_{c.m.}=1.99$ MeV ($J^{\pi}=0^{+}$) resonance and the resonance strength of the $E_{c.m.}=1.054$ MeV ($J^{\pi}=1^{-}$) resonance are reported. The astrophysical S factor for nonresonant capture into the ^{20}Ne ground state was measured to be 0.26 ± 0.07 MeV b, assuming an energy-independent S factor between $E_{c.m.}=1.7$ and 2.35 MeV. Using theoretical estimates for the energy dependence and branching ratios for the nonresonant capture, a best estimate for the total S factor at 300 keV of 0.7 ± 0.3 MeV b is determined.

I. INTRODUCTION

The $^{16}O(\alpha,\gamma)^{20}Ne$ reaction is expected to occur during the helium burning stage of stellar evolution. It is helium burning that provides the bridge over the instability gaps at mass 5 and mass 8 in stellar nucleosynthesis through the triple alpha reaction, $^{8}Be(\alpha,\gamma)^{12}C$, and determines the relative abundance of ^{12}C to ^{16}O through the $^{12}C(\alpha,\gamma)^{16}O$ reaction. The subsequent capture of an alpha particle by ^{16}O to form ^{20}Ne is thought to occur at too slow a rate[1] to affect either the ^{16}O or ^{20}Ne abundance significantly. However, recent calculations using a microscopic cluster model[2] and the generator coordinate method[3] have yielded a reaction rate at helium burning energies four to five times larger than that recommended previously.[1] Even though this change should not significantly alter the astrophysical predictions,[4] experimental measurements are crucial in order to test the range of validity of these new calculations, as they also play a key role in determining the astrophysical rates[5] of experimentally inaccessible reactions.

At the typical helium burning temperatures of 2–3×10^{8} K (corresponding to an effective energy for helium burning reactions of $E_{c.m.}\sim0.300$ MeV), the $^{16}O(\alpha,\gamma)^{20}Ne$ reaction rate is dominated by nonresonant direct capture, while at higher temperatures, resonant capture through several known low-energy resonances is also possible. A level scheme for ^{20}Ne is shown in Fig. 1, where only those states relevant to $^{16}O(\alpha,\gamma)^{20}Ne$ are indicated. The parameters for the important resonances have been determined experimentally, but the contribution from the direct capture has previously been determined by theoretical calculation alone.

From the recent predictions of the direct capture cross section,[2,3] it appeared possible that the direct capture could be observed at center-of-mass energies of ~1.6–2.5 MeV. While higher than energies of stellar interest, measurements here can establish the magnitude of the nonresonant capture process, allowing a reliable extrapolation to stellar energies. In fact, for carefully chosen energies, the direct capture cross section was expected to exceed the contribution from narrow resonances. The $J^{\pi}=1^{-}$ resonance at $E_{c.m.}=1.054$ MeV, the $J^{\pi}=3^{-}$ resonance at $E_{c.m.}=2.429$ MeV, and other nearby resonances contribute little to the cross section at these energies, because they are either too narrow or too weak. However, the $J^{\pi}=0^{+}$ resonance at $E_{c.m.}=1.99$ MeV was expected to contribute significantly to the cross section at the energies of interest. Thus a more accurate measurement of the width and strength of this $J^{\pi}=0^{+}$ resonance was necessary in order to determine the direct capture contribution to the total cross section. Data were also taken at the 1^{-} and 3^{-} resonances for calibration purposes and to study system parameters.

A new coincidence technique was used in the present experiment, where both the γ ray and the ^{20}Ne recoil particle from the reaction were detected. When used in conjunction with an efficient recoil separator and a recoil detector capable of distinguishing ^{20}Ne recoils from background ^{16}O beam particles, the requirement of time-of-flight coincidence can provide an essentially background-free signature of the $^{16}O(\alpha,\gamma)^{20}Ne$ reaction.

II. EXPERIMENTAL PROCEDURE

The 3 MV Pelletron Tandem Accelerator at the Kellogg Radiation Laboratory was used to provide high current ^{16}O beams from a Cs sputter source. Beam currents incident on the target were typically several particle μA. The beam energy was defined and stabilized with slits before and after a 90° analyzing magnet. The analyzing magnet was calibrated at the narrow 1^{-} resonance in $^{16}O(\alpha,\gamma)^{20}Ne$, which has a known center-of-mass energy[6] of 1.0539 ± 0.0018 MeV.

The apparatus, which included a transmission gas target and an electromagnetic recoil separator, is shown schematically in Fig. 2. The target was a differentially pumped, 5.72 cm diameter cylindrical chamber which was pressurized to 2.5 Torr of high-purity (99.999%) helium gas. The amount of gas outside of this central

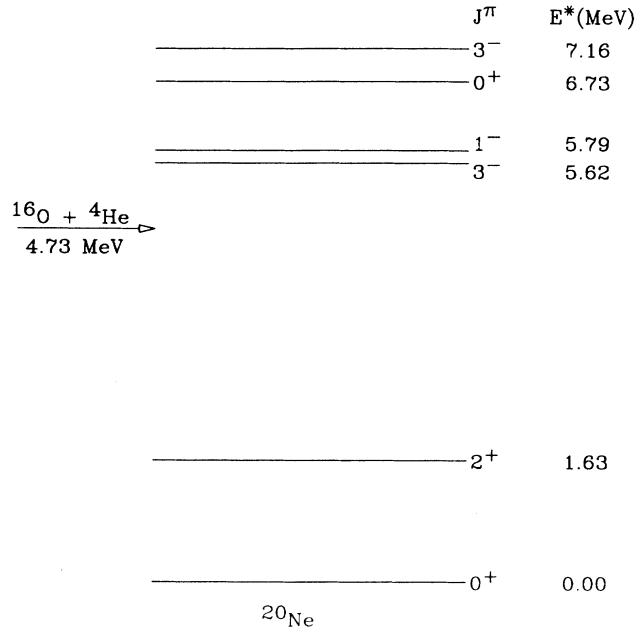

FIG. 1. Level diagram of ^{20}Ne showing the natural parity states which are relevant to $^{16}O(\alpha,\gamma)^{20}Ne$.

chamber (i.e., in the 10 cm diameter differential pumping stage) amounted to $\sim 10\%$ of the total target thickness. Since both the γ-ray efficiency and the recoil detection efficiency are essentially independent of position in this region, the total target thickness was used in the analysis. The pressure was reduced to the vacuum of the beamline by a series of small apertures and high speed pumps. The target thickness was determined to be $(5.4\pm0.2)\times10^{17}$ particles/cm^2 for 2.5 Torr of target pressure by measuring the energy loss through the target for several (α,γ) resonances with ^{12}C and ^{16}O beams. It was also measured using the energy loss of a proton beam measured with the 0.992 MeV resonance in the $^{27}Al(p,\gamma)^{28}Si$ reaction with an aluminum target placed after the ^{4}He target. The main uncertainty in the target thickness arises from the uncertainties in the stopping powers.[7]

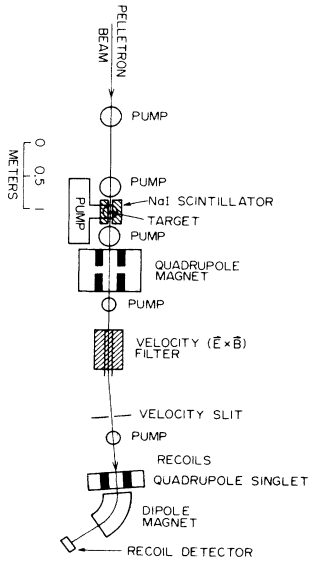

FIG. 2. Schematic diagram of the experimental apparatus.

To detect elastically scattered alpha particles for beam current normalization, a silicon surface barrier detector was placed 6.3 cm from the center of the target. The silicon detector was placed at an angle of 60° from the beam axis, and its acceptance was defined by a 0.5 mm collimator in front of the detector. The total number of incident ^{16}O ions at each energy was determined through a two-step calibration of the number of elastically scattered alpha particles detected in the silicon detector. This two-step calibration is required because the α particle yield in the vicinity of a resonance can deviate significantly from the Rutherford cross section. Calibrating the alpha particle yield directly against the integrated charge of the beam after the target was not possible, since the gas in the target equilibrated the single incident charge state of the beam into a distribution. Instead, the alpha particle yield was calibrated against the integrated beam power of the ^{16}O beam by attaching a beam power calorimeter[8] to the beamline downstream from the target. The calorimeter provided a dc current proportional to the incident beam power, and the integrated output current was therefore proportional to the beam energy times the total number of particles. The beam power calorimeter was then calibrated against the number of incident particles by repeating the measurement without gas in the target and using electrical beam current integration. The uncertainty in the number of incident particles determined with this procedure was $\pm5\%$.

Four large NaI(Tl) crystal scintillators ($15.2\times15.2\times25.4$ cm) were used for γ-ray detection. Placed in close geometry to the target, their total efficiency was over 50% in the energy range of interest. The NaI(Tl) crystals provided both energy and timing signals. The energy resolution was measured to be 9% for 0.661 MeV γ rays from ^{137}Cs, and the timing resolution was measured to be 4.5 nsec for the ^{60}C γ-ray cascade with a plastic scintillator start channel. Five centimeters of lead and 1.3 cm of plastic scintillator surrounded the NaI(Tl) crystals to reduce the background rate from cosmic rays and natural radioactivity.

^{20}Ne recoils produced from the reaction were separated from the incident ^{16}O beam by a recoil separator, composed of a quadrupole doublet, a Wien ($\mathbf{E}\times\mathbf{B}$) velocity filter for velocity separation, a quadrupole singlet, and a 60° dipole magnet for momentum/charge (p/q) separation. The recoil separator was tuned to maximize the transmission of an abundant charge state of recoils from the gas target and to minimize the beam-induced background. The Wien filter provided the bulk of the separation of the ^{20}Ne recoils from the main beam by directing the incident beam to a beam dump while transporting the ^{20}Ne recoils to a set of velocity slits. The ve-

locity slits were centered 3° from the incident beam direction with the additional deflection of the recoils resulting from extended electric field plates in the Wien filter. This deflection provided for rejection of neutral background particles that are not deflected by the Wien filter. The dipole magnet following the velocity slits provided further background reduction and, combined with the quadrupole singlet, imaged the recoils onto the recoil detector.

Because a ^{20}Ne beam could not be produced at the appropriate energies, the recoil separator was tuned with reaction ^{20}Ne ions and by extrapolation from settings determined with ^{16}O and ^{19}F beams over the energy range of the experiment. The quadrupole and dipole magnets were scaled in p/q directly from the optimal settings for ^{16}O and ^{19}F beams; however, because of coupling between the electric and magnetic fields in the Wien filter, a calculation (based on the electric and magnetic rigidities of the beam and the effective lengths of the electric and magnetic fields) was used to semiempirically predict its settings. ^{19}F and ^{16}O beams at various energies and charge states were used to determine the parameters of the code. For a single incident beam momentum, the magnetic field in the Wien filter was varied to maximize transmission of the beam through the velocity slits at different electric field settings, and the parameters of the code was adjusted to reproduce the measurements. ^{20}Ne recoils from the $J^{\pi}=1^{-}$, $J^{\pi}=0^{+}$, and $J^{\pi}=3^{-}$ resonances were also used to verify that the settings were accurately predicted for c.m. energies between 1.054 and 2.429 MeV. The velocity slits after the velocity filter were set to a width of ± 1.0 cm, corresponding to a velocity acceptance of $\sim \pm 2.0\%$. A Monte Carlo beam optics code based on TRANSPORT (Ref. 9) showed that, with this acceptance, there would then be 100% transmission of ^{20}Ne recoils from ^{16}O$(\alpha,\gamma)^{20}$Ne through the recoil separator over the entire energy range of the experiment. This was confirmed at the peak of the strong resonances by measuring the ratio of the coincidence yield to the singles γ-ray yield which, with 100% transmission, should equal the charge state fraction of the selected recoil.

The recoil particle detector consisted of a dual gas ionization chamber of isobutane separated from the beamline by an ~ 40 μg/cm^2 thick, 3.8 cm diameter polypropylene window. The recoil detector provided three separate signals. The first was a fast timing signal, produced from a thin (5 mm thick) low-pressure multiwire proportional chamber[10] which was filled with 1 Torr of isobutane and run at 400 V on the anode wire plane. The measured timing resolution was 2.5 nsec, measured with alpha particles from an ^{241}Am source. The remaining signals were differential energy (ΔE) and residual energy ($E-\Delta E$) signals from two insulated collector plates located in the second chamber through which 6–8 Torr of isobutane continuously flowed. Since ^{16}O and ^{20}Ne ions have different stopping powers over the energy range of interest, they could be distinguished in the resulting two-dimensional E-ΔE spectra.

Data were collected event-by-event through an analog to digital converter (ADC) which began conversion when a γ ray with $E_{\gamma} \geq 1.3$ MeV was detected in any of the NaI(Tl) detectors. However, the ADC was automatically cleared unless a fast signal from the recoil detector was received within 1.5 μsec after the γ-ray detection, since the ^{20}Ne recoil time-of-flight between the target and the recoil detector was always less than 1 μsec. If not cleared, the output from the ADC was processed on a VAX 11/750 and later transferred to tape. The pulse heights recorded for each event were from each of the four NaI(Tl) crystals, E and ΔE signals from the recoil detector, and the time interval between γ ray and recoil particle detection. The singles rates in the detectors were $\sim 15-30$ kHz in the recoil detector and ~ 100 Hz in the NaI(Tl) detectors, resulting in a trigger rate of several Hz.

Data were taken at energies corresponding to the above-mentioned 1^{-}, 0^{+}, and 3^{-} resonances in the ^{16}O$(\alpha,\gamma)^{20}$Ne reaction, and at four off-resonance energies, $E_{\text{c.m.}}=1.7$, 2.2, 2.3, and 2.35 MeV. Detailed excitation functions were measured at the three resonances for target thickness information and to study systematics. These measurements were done at a target pressure of 1 Torr in order to improve the sensitivity to the resonance widths of the 0^{+} and 3^{-} resonances. For high statistics, the reaction was run at the peak of each resonance until several thousand ^{20}Ne γ-ray coincidences were detected. The theoretical predictions of Langanke[2] indicated that the direct capture would be significantly higher than the residual resonance contributions at each of the four nonresonant energies, and data were taken at these energies until ~ 100 ^{20}Ne γ-ray coincidences were observed. As expected, the run at 1.7 MeV had the lowest cross section and consumed almost 40 h of running time.

The efficiency of the apparatus is mainly the product of three separate efficiencies: the charge state fraction of the reaction ^{20}Ne, the NaI(Tl) detection efficiency within the selected γ-ray energy cuts, and the E-ΔE recoil detection efficiency.

Since a ^{20}Ne beam at the appropriate energies was not available from the accelerator, the ^{20}Ne charge state fraction was determined by fitting a semiempirical formula to charge state distributions measured with ^{16}O, ^{19}F, and ^{23}Na beams incident on the ^{4}He gas target. It has been shown[11,12] that a reasonably good description of charge state distributions can be obtained with the following Gaussian parametrization for the fraction of a given charge in an equilibrium distribution,

$$F_i=(2\pi\sigma^2)^{-(1/2)}e^{-(i-i_0)^2/2\sigma^2}, \quad (1)$$

where the mean charge is $i_0=\kappa v Z_i+C$, and the width of the Gaussian is $\sigma=\sigma_0 Z_i^{1/2}$. Z_i is the atomic number of the incident particle, v is the velocity of the incident particle, and κ, C, and σ_0 are semiempirical parameters. ^{16}O charge state fractions were measured over the energy range of the experiment by placing a cup connected to an electrical integrator after the dipole magnet in the recoil separator. The dipole magnet was set to select individual charge states, and the fractions were determined by comparing the integrated currents in the cup to the

alpha particle yield in the silicon detector. These data were then fitted to the above parametrization in order to calculate the charge state distributions for other incident ions. Further measurements of charge state fractions for ^{19}F and ^{23}Na, over a narrower energy range, were then performed to verify that the charge state predictions were valid. The fit to the ^{16}O data and the prediction for ^{19}F are shown in Fig. 3 along with the measured data. Predictions for ^{23}Na also agreed with the measurements to better than 5%. The above parametrization also agreed with previous measurements[13] of ^{20}Ne on ^{4}He to within 5%. We have assigned a total error of 10% to the predicted ^{20}Ne charge state fractions, as this is the level of agreement found in previous studies of the Gaussian model, and we have also found that the fit to the ^{16}O measurements requires this magnitude of uncertainty in the data to achieve a χ^2_ν of 1.0.

The parametrization of the charge state fractions with Eq. (1) depends to a large extent on the attainment of equilibrium for the charge state distribution. Equilibrium can be obtained with a sufficiently thick target and can be checked by measuring the charge state fractions as a function of target thickness. We have performed such measurements by varying the pressure in the gas target, and find that at 2.5 Torr the target is ~ 5 times equilibrium thickness. There is thus a potential nonequilibrium distribution of charge states for ^{20}Ne recoils produced in the last 20% of the target. However, we have performed detailed calculations of the approach to equilibrium using the energy dependence of the electron pickup and loss cross sections which indicate that this effect produces charge state fractions which differ from equilibrium by $<5\%$. Measurements of reaction yields at different target pressures confirm this estimate.

The total NaI(Tl) efficiency was measured for an isotropic γ-ray distribution using the $E_p = 340$ keV resonance in the ^{19}F(p,$\alpha\gamma$)^{16}O reaction. Since there is nearly a one to one ratio of emitted alpha particles to 6.13 MeV γ rays produced in the reaction, the NaI(Tl) efficiency

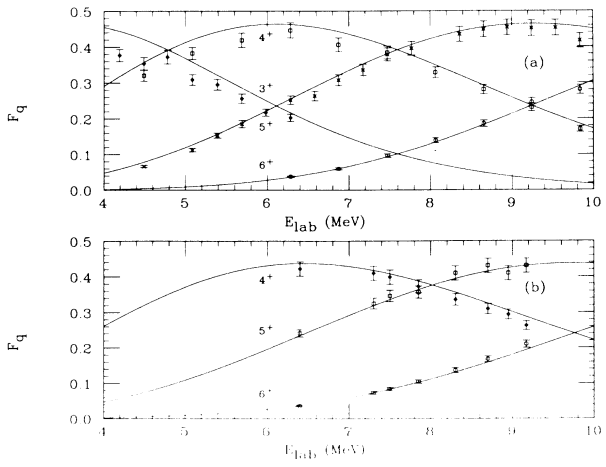

FIG. 3. Measured charge state fractions: (a) ^{16}O data and the fit from Eq. (1); (b) predicted charge state fractions for ^{19}F and measured values.

was extracted by determining the geometric acceptance of a silicon surface barrier detector, which detected the alpha particles from the reaction. With this technique the total absolute efficiency of the four NaI(Tl) detectors at $E_\gamma = 6.13$ MeV was measured to be 58 ± 2 %. The relative detection efficiency at low energies was measured with radioactive sources and at higher energies with the 4.44 and 11.66 MeV γ rays from the ^{11}B(p,γ)^{12}C reaction at $E_p = 163$ keV. The NaI(Tl) efficiency for nonisotropic γ-ray angular distributions was calculated from the detector geometry. This calculation involved an integration of the γ-ray absorption over all possible paths between the source and the detectors as well as the absorption in the material surrounding the target. The large angular range accepted by the detectors reduced the importance of this effect. The calculated efficiencies for pure $E1$ and $E2$ capture to the ground state were 67% and 56%, respectively.

The γ-ray efficiency for a particular window on the γ-ray energy was determined at 4.44 and 11.66 MeV by using the $E_p = 163$ keV resonance in ^{11}B(p,γ)^{12}C. These γ rays are produced in cascade from the 16.1 MeV resonant state. Thus by demanding a γ-γ coincidence between the detectors, the response of the individual detectors to a single γ ray at these two energies can be determined with little background. It was found that for a low energy cut of $0.6E_\gamma$ the efficiency of the energy cut was nearly independent of γ-ray energy and amounted to 0.74 ± 0.02.

Because of the very large detection efficiency of the NaI(Tl) detectors, a correction of the yields for summing of the pulse heights from coincident γ rays is required. This was accomplished by comparing the net yields for various combinations of the addition of the pulse heights from the four detectors. By comparing the yields from a single detector with those with any pair, any three, and all four added together, the amount of summing-in or summing-out could be determined.

The recoil detector inefficiency resulted from ions hitting the wires in the timing detector, and from pileup due to the high rate in the detector. The efficiency was analyzed at several resonances in ^{16}O(α,γ)^{20}Ne as a function of the rate in the detector. This was done by producing two time-of-flight (TOF) spectra, one generated with a cut on the selected window in the E-ΔE spectrum, and the other without a cut. The ratio of the coincident yields from the two spectra determined the efficiency of the recoil detector. A 5% inefficiency observed at very low rates was consistent with the fraction of the aperture obscured by the wires in the timing detector. At 30 kHz, the highest rate used, the total efficiency of the recoil detector was 0.77 ± 0.05.

III. ANALYSIS AND RESULTS

Yields were extracted during replay of the data by generating TOF spectra with a window on the ^{20}Ne peak in the E-ΔE spectra and a window on the desired γ-ray energy in the NaI(Tl) detectors. Examples of these TOF spectra are shown in Fig. 4. Because of the large efficiency of the NaI(Tl) detectors, summing of cascade γ

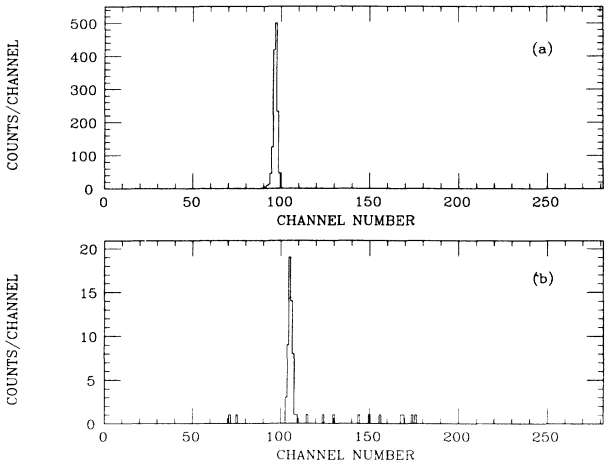

FIG. 4. Time-of-flight spectra for γ-ray and recoil ^{20}Ne coincidence from the $^{16}O(\alpha,\gamma)^{20}Ne$ reaction: (a) $E_{c.m.}=1.99$ MeV; (b) $E_{c.m.}=1.70$ MeV. The abcisssa corresponds to 7 nsec per channel.

rays can pose a serious problem if the pulse heights from the detectors are simply added. To correct for this effect, TOF spectra were created requiring a γ ray within the desired energy window in any one detector, in any pair of detectors, in any triplet of detectors, and finally in all four detectors. By extrapolating these yields to zero detector number, a zero-summing yield is obtained.

The excitation energy E^* in ^{20}Ne is the Q value for the reaction (4.731 MeV) plus the c.m. energy, which ranged between 1.05 and 2.35 MeV. For all of the measured energy range, except near the 3^- resonance, the reaction γ rays are expected either to cascade through the $E^*=1.63$ MeV, $J^\pi=2^+$ first excited state in ^{20}Ne or to decay directly to the ground state. The 0^+ resonance is expected to decay $\sim 100\%$ of the time through the 1.63 MeV state since the ground state is also 0^+. Two separate TOF spectra were generated at each beam energy: one with a minimum cut on the γ-ray energy above the 1.63 MeV transition, and another with a minimum cut above $E^*-1.63$ MeV. The total yield was extracted from the first cut and the ground state contribution from the second cut.

In order to determine the resonance widths and strengths, the resonance excitation functions were fitted to an integrated Breit-Wigner resonance shape including beam energy spread, energy straggling, and the stopping power of the target. Fitting the narrow 1^- resonance ($\Gamma_T=28$ eV[6]) provided the beam energy spread and straggling parameters for the fits to the other resonances. Since the widths of the 0^+ and 3^- resonances with the dominant effect determining the shape of the leading and trailing edge of the excitation function, uncertainties in beam energy spread, beam straggling, and target thickness contributed little to the uncertainty in the extracted widths. The data taken in the 1^- and 0^+ resonances, together with the fits, are shown in Fig. 5. The measured total widths of the 0^+ and 3^- are in good agreement with previous values (see Table I).

Since the target thickness (~ 45 keV at 2.5 Torr target pressure) at the energy of the 1^- resonance was much greater than the resonance width of the state ($\Gamma\sim 28$ eV), the 1^- resonance strength was calculated using the thick target equation:

$$\omega\gamma = \text{yield}\left[\frac{A_t}{A_t+A_i}\right]^2 \frac{M_i E_r \epsilon_\alpha}{\pi^2\hbar^2 N_i \epsilon_T}\ , \tag{2}$$

where $\omega\gamma$ is the c.m. resonance strength, A_i and A_t are the atomic numbers of the incident and target particles, M_i is the mass of the incident particle, E_r is the c.m. resonance energy, ϵ_α is the stopping power per atom per cm^2 of the target at the lab energy of the beam, N_i is the number of incident particles, and ϵ_T is the total detection efficiency. The measured strength of the resonance was 19.7 ± 4.1 meV, compared to previous values[14,15] of 12 ± 3 and 18.2 ± 3 meV. The measured ground state branching ratio of $19\pm 4\%$ is in good agreement with the previous value[6] of $18\pm 5\%$.

For the determination of the resonance strength of the 0^+ state, data were taken at two different target pressures: 1.0 and 2.5 Torr. This provided an important check because the target thickness was not much greater than the expected natural width of the state. From a thin target analysis the resonance strengths as measured with both target pressures agreed to $<5\%$ and yielded an average value of 71 ± 12 meV. The measured resonance parameters are compared with previous data in Table I.

There is some disagreement between the previous work and this experiment for the resonance strength of the 0^+ transition. Both of the previous experiments[14,15] employed a SiO_2 target with an incident ^{4}He beam, and both reported a difficulty posed by a nearby resonance in $^{18}O(\alpha,n)^{21}Ne$ at $E_{c.m.}=1.975$ MeV, arising from the naturally occurring ^{18}O impurities in the SiO_2. The

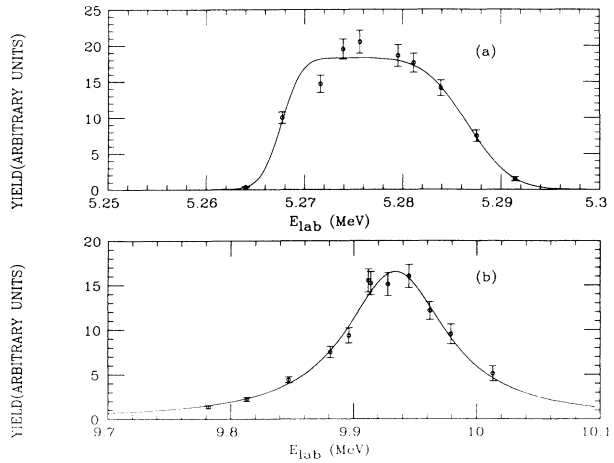

FIG. 5. Coincidence excitation function for two resonances in $^{16}O(\alpha,\gamma)^{20}Ne$: (a) $J^\pi=1^-$, $E_{c.m.}=1.05$ MeV; (b) $J^\pi=0^+$, $E_{c.m.}=1.99$ MeV.

TABLE I. Total widths and resonance strengths of states in ^{20}Ne studied in the ^{16}O$(\alpha,\gamma)^{20}$Ne reaction.

$E_{c.m.}$ (MeV)	E^* (MeV)	J^π	$\Gamma_{c.m.}$ (keV) Present	$\Gamma_{c.m.}$ (keV) Previous	$\omega\gamma_{c.m.}$ (meV) Present	$\omega\gamma_{c.m.}$ (meV) Previous
1.055	5.785	1^-		$(2.8\pm0.3)10^{-2}$	20±4	14 ±3
1.994	6.722	0^+	20 ±3	15 ±7	71±12	38 ±10
2.432	7.156	3^-	8.3±0.5	8.1±0.3		11.3±1.3

^{18}O$(\alpha,n)^{21}$Ne reaction complicated their analysis, and it is possible that this neutron background may have introduced a large systematic error in their yield extractions. It was noted in Ref. 15 that their measured $E2$ transition strength for the decay of this resonance was about a factor of 4 lower than other $E2$ intraband transitions in ^{20}Ne. The present measurement reduces this discrepancy somewhat.

The measured resonance parameters were then used to calculate the energy dependence of the resonance cross sections in the single-level R-matrix approximation,[16] and the calculated cross sections were then compared with the measured cross sections at the off-resonance energies to search for a nonresonant contribution to the cross section. As expected, the calculated resonance cross sections at 1.7, 2.2, 2.3, and 2.35 MeV yield significant contributions only from the 0^+ resonance. The calculated resonance cross section and the measured cross sections are shown in Fig. 6. This calculation assumed a radius of 6.0 fm. Variation of this parameter by ±0.5 fm changes the calculated cross section at 1.7 MeV (the most sensitive energy) by ±12%. As can be seen in the figure, the measured cross section is significantly larger than the resonance contribution both below and above the 0^+ resonance, indicating the presence of nonresonant capture. However, the extraction of the nonresonant cross section is complicated by the possibility of interference with the resonant amplitude for capture from the same partial wave. The calculations of Langanke[2] and Descouvemont and Baye[3] predict that the nonresonant capture proceeds predominantly by a cascade through the 1.63 MeV 2^+ state from initial states with $l=0$, 2, and 4. Nonresonant radiative capture from the initial s wave will interfere with the 0^+ resonance capture, which complicates the determination of the nonresonant capture cross section. However, 20–25 % of the total nonresonant capture is predicted to be from the initial $l=2$ state directly to the ground state. As the 0^+ resonant capture is a pure cascade (branching ratio >98% from the present experiment) through the 2^+, 1.63 MeV state, the contribution to the ground state capture from the 0^+ resonance should be negligible. The $E2$ ground state component of the nonresonant capture can thus be determined without interference from resonance contributions, at the off-resonance energies.

The ground state cross sections were analyzed in terms of the astrophysical S factor:

$$S(E_{c.m.})=E_{c.m.}\sigma(E_{c.m.})e^{(E_G/E_{c.m.})^{1/2}}, \quad (3)$$

where E_G is the Gamow energy [$E_G=(2\pi\alpha Z_1 Z_2)^2\mu c^2/2$; μ is the reduced mass of the incident channel, and α is the fine structure constant].

The measured S factor for capture into the ground state of ^{20}Ne is shown in Fig. 7. Because the S factor is expected to be nearly independent of energy for the energy range of the measurements, a weighted average can be taken, yielding a result for S of 0.26±0.07 MeV b for $E_{c.m.}=1.7$–2.35 MeV. This is significantly lower than the value of ~1.2 MeV − b predicted by Langanke[2] for d-wave capture to the ground state. The calculation of Descouvemont and Baye[3] predicted a total d-wave capture (both to the ground and first excited state) of ~0.8 MeV − b in the energy range of the present experiment.

As discussed above, it was not possible to determine the total nonresonant S factor in the present experiment because of the potential interference between the 0^+ resonance yield and the cascade component of the nonresonant capture. However, upper limits on the nonresonant cross section can be set by assuming that the interference is such that the nonresonant capture is as large as possible but still consistent (at the $2-\sigma$ level) with the measured cross section. The upper limits for the total nonresonant capture S factor are calculated to be 2.3 MeV b at $E_{c.m.}=2.35$ MeV and 2.8 MeV b at $E_{c.m.}=2.3$ MeV with >95% confidence. These upper limits were set for the case of fully destructive interference above the 0^+ resonance, and are just barely consistent with the theoretical calculations.[2,3] Perhaps the

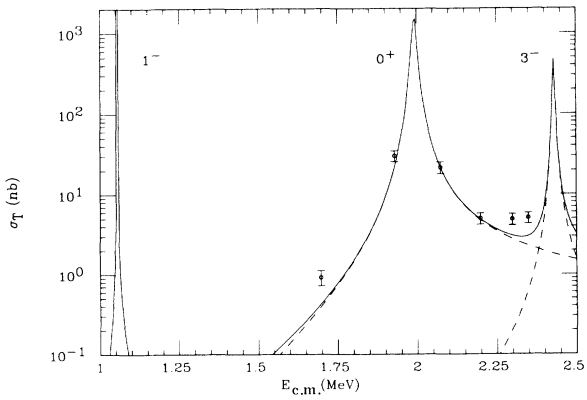

FIG. 6. Measured total cross sections for ^{16}O$(\alpha,\gamma)^{20}$Ne. The dashed curves are the calculated individual resonance contributions (with J^π as indicated) and the solid curve is the sum of these contributions.

best way to estimate the S factor at the astrophysically interesting energy of $E_{c.m.} \sim 300$ keV is to use the measured value for ground state capture, and the theoretical predictions for the branching ratios and energy dependence. Such an analysis yields a total S factor of 0.7 ± 0.3 MeV b, where an additional uncertainty of 30% has been added in quadrature to account for the differences in the energy dependence predicted by the two calculations. We note that this best estimate is approximately a factor of 2 larger than the older estimates[1] for S (300 keV).

While this new value for S (300 keV) should not significantly alter our understanding of nucleosynthesis during helium burning, the experiment provides an important constraint on the theoretical calculations of reaction rates. Such calculations must be verified where experimental information is available in order to reliably predict rates for reactions that are inaccessible to experiment: cases of very small cross sections, nuclear physics complications, or very short-lived nuclei.

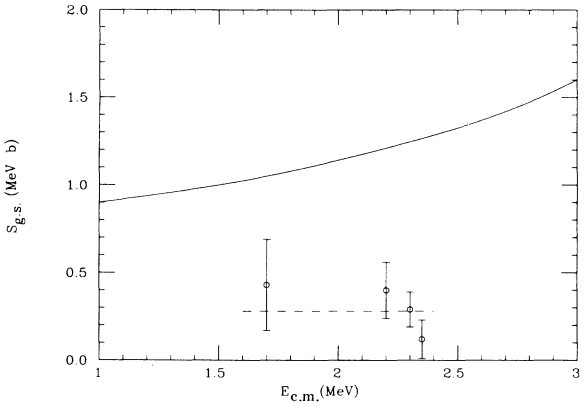

FIG. 7. S factor for capture into the ^{20}Ne ground state. The solid curve is the prediction of Langanke (Ref. 2). The dashed line is the weighted average of the measured values.

ACKNOWLEDGMENTS

The authors would like to thank C. A. Barnes, W. A. Fowler, R. M. Kremer, and K. Langanke for many helpful discussions, and S.-C. Wu for assistance during part of the data acquisition. This work was supported in part by a gift to the California Institute of Technology from the W. M. Keck Foundation and by National Science Foundation Grant PHY 85-05682.

*Present address: Department of Physics, Stanford University, Stanford, CA 94305.
†Present address: AT&T Bell Laboratories, Norcross, GA 30071.
‡Present address: Department of Physics, Ohio State University, Columbus, OH 43210.

[1]W. A. Fowler, G. R. Caughlan, and B. A. Zimmerman, Annu. Rev. Astron. Astrophys. **13**, 96 (1975).
[2]K. Langanke, Z. Phys. A **317**, 325 (1984).
[3]P. Descouvemont and D. Baye, Phys. Lett. **127B**, 286 (1983).
[4]W. A. Fowler, private communication.
[5]B. W. Filippone, Annu. Rev. Nucl. Part. Sci. **36**, 717 (1986).
[6]F. Ajzenberg-Selove, Nucl. Phys. **A392**, 1 (1982).
[7]H. H. Andersen and J. F. Ziegler, *The Stopping and Ranges of Ions in Matter* (Pergamon, New York, 1977), Vols. 3 and 5.
[8]J. L. Osborne and A. J. Howard, Nucl. Instrum. Methods Phys. Res. **222**, 428 (1984).
[9]K. L. Brown, F. Rothacker, D. C. Carey, and Ch. Iselin, Stanford Linear Accelerator Center Report 91, 1977, Revision 2 (unpublished).
[10]A. Breskin, Nucl. Instrum. Methods **141**, 505 (1977); A. Breskin, R. Chechik, and N. Zwang, *ibid* **165**, 125 (1979).
[11]V. S. Nikolaev, Usp. Fiz. Nauk **85**, 679 (1965) [Sov. Phys. Usp. **8**, 269 (1965)].
[12]A. B. Wittkower and G. Ryding, Phys. Rev. **4**, 226 (1971).
[13]A. B. Wittkower and H. D. Betz, At. Data **5**, 113 (1973).
[14]C. Van der Leun, D. M. Sheppard, and P. J. Smulders, Phys. Lett. **18**, 134 (1965).
[15]J. Toevs, Nucl. Phys. **A172**, 589 (1971).
[16]A. M. Lane and R. G. Thomas, Rev. Mod. Phys. **30**, 269 (1958).